Available online at BCREC website: https://bcrec.id

Bulletin of Chemical Reaction Engineering & Catalysis, 17 (3) 2022, 533-541

Research Article

Biomass Valorization to Chemicals over Cobalt Nanoparticles on SBA-15

Wega Trisunaryanti*, Triyono Triyono, Elizabeth Selia Nandini, Endah Suarsih

Department of Chemistry, Universitas Gadjah Mada, Sleman, DI Yogyakarta, Indonesia.

Received: 13th July 2022; Revised: 3rd August 2022; Accepted: 3rd August 2022
Available online: 7th August 2022; Published regularly: September 2022

Abstract

A series of heterogeneous catalysts based on cobalt supported on SBA-15 were prepared through wet impregnation and co-impregnation assisted by ethylene glycol (EG) methods. The cobalt oxide catalysts generated after the drying and calcination process were denoted as CoO/SBA-15w and CoO/SBA-15c for a wet- and co-impregnation method, respectively. Subsequent to the reduction process, the reduced cobalt catalysts were obtained and denoted as Co/SBA-15w and Co/SBA-15c. The TEM images revealed the catalysts prepared through these methods show very clear distinctions that the catalyst prepared by wet impregnation shows large aggregates of cobalt particles on the external surface of SBA-15 due to their inability to enter the channels. The catalysts were evaluated on the hydrocracking of pyrolyzed α-cellulose as a biomass model. The results showed that the reduced cobalt-based catalysts are having higher conversion value and selectivity towards the 2-furancarboxaldehyde reached *ca.* 20%.

Keywords: Hydrocracking; α-cellulose; heterogeneous catalyst; cobalt; SBA-15

How to Cite: W. Trisunaryanti, T. Triyono, E.S. Nandini, E. Suarsih (2022). Biomass Valorization to Chemicals over Cobalt Nanoparticles on SBA-15. *Bulletin of Chemical Reaction Engineering & Catalysis*, 17(3), 533-541 (doi: 10.9767/bcrec.17.3.15160.533-541)

Permalink/DOI: https://doi.org/10.9767/bcrec.17.3.15160.533-541

1. Introduction

The demand for chemicals is gradually increasing in modern life as it serves as raw materials for the production of commodities such as drugs, preservatives, fibers, and paints. In this sense, the conversion of biomass into renewable chemicals and fuels has gained much attention as it is one of the keys to a sustainable society [1–8]. However, the use of edible carbohydrates as a biomass source for chemical manufacture has resulted in a food corps competition [9]. The use of lignocellulosic biomass could address this problem as it serves as a potential source of sustainable feedstock and fuels [10]. Cellulose is expected to be the first target for a chemical resource from biomass because cellulose is an inedible carbohydrate [9]. It can serve as precursor material to generate high-value utilization chemicals such as furfural with a wide variety of transformation routes to further synthesize higher-value chemicals such as furan dicarboxylic acid (FDCA), furfuryl amine, furfuryl alcohol, and others [11].

Cellulose can be converted into bio-oils through the thermochemical processes (pyrolysis, gasification, liquefaction, and high-pressure supercritical extraction) which are considered simpler and lower-cost operations [12]. This kind of transformation offers unique advantages for the formation of fuels and important chemicals in the industries [13,14]. In this case, pyrolysis is proven to be one of the most promising methods to convert biomass into several products, such as: syngas, bio-liquid,

* Corresponding Author.
Email: wegats@ugm.ac.id (W. Trisunaryanti);
Telp: +62 274 545188

char, and chemicals [15]. However, due to the low quality and complicated composition, products are typically obtained with very low yield and purity. For this reason, the conversion of cellulose requires effective catalytic systems and the exploration of a catalyst with excellent activity and stability is continuing.

To improve the conversion efficiency, the selection of metals and support as the catalyst has become a key factor [16]. For instance, mesoporous catalyst supports, such as SBA-15 with high specific surface area, excellent thermal stability, tunable porosity, and uniform hexagonal pores, and thick pore walls, can improve the biomass conversion due to their active sites, high thermal/hydrothermal stability, and enhanced shape selectivity [17–20]. In this sense, dispersing active metal(s) on the mesoporous support would be beneficial to improve the conversion process as it can depress the catalyst deactivation during the harsh reaction condition [21]. Moreover, designing a catalyst with strong metal-support interactions with good confinement of metal particles will be plausible.

Our group has previously demonstrated [22] that the impregnation of nickel on SBA-15 assisted by polyol could enhance the selectivity towards the formation of hydrocarbons due to the formation of a branched alkane in the hydrocracking of pyrolyzed α-cellulose. In addition, the nickel-based catalyst also showed excellent stability in the dry reforming of methane with CO_2 to produce syngas and hydrogen [23]. Moreover, the polyol-assisted preparation method is reported to have provided more active sites for reaction due to the high dispersion of metal particles and excellent coke resistance [24–26] Based on these considerations, we aim to make use of cobalt as another base metal alternative to be evaluated for the hydrocracking of pyrolyzed α-cellulose. The nature and the dispersion of cobalt are the key factors to determine the activity and the selectivity of the supported catalyst [27]. Another study [28] reports that cobalt has emerged as an active metal catalyst for C−C bond scission that is beneficial for cracking reactions.

In this regard, the hydrocracking of pyrolyzed α-cellulose will allow to diversify the approach for biomass valorization to produce the value-added chemicals. The alternative design of catalyst is crucial to enhance its performance. In this study, cobalt supported on SBA-15 catalysts were prepared through wet and co-impregnation using ethylene glycol (EG). The catalysts were evaluated of the hydrocracking of pyrolyzed α-cellulose as a model of biomass.

2. Materials and Methods

2.1 Catalyst Preparation

The SBA-15 support material was from Green Stone Swiss Co. Ltd. and $Co(NO_3)_2 \cdot 6H_2O$ as a salt precursor was supplied by Merck. 10% of cobalt supported on SBA-15 catalysts was prepared by the wet and co-impregnation method. The latter method used a defined amount of ethylene glycol supplied by Merck (Co/EG molar ratio = 1) during the dissolution of the salt precursor. The mixtures were stirred and dispersed on the SBA-15 support, consequently settled overnight, evaporated, and finally dried at 100 °C. Afterward, the dried solids were calcined at 500 °C for 5 hours in the air. The obtained solids were denoted as CoO/SBA-15w and CoO/SBA-15c. Thereafter, the solids were reduced by H_2 gas stream (20 mL/min) provided by PT. Samator Indonesia with 99.00% purity at 400 °C for 3 hours to obtained Co/SBA-15w and Co/SBA-15c.

2.2 Catalyst Test

The prepared catalysts were evaluated for the hydrocracking of pyrolyzed α-cellulose. It was carried out by using a stainless-steel semi-batch cracking reactor tube with an inner diameter of 2.80 cm, an outer diameter of 3.10 cm, and a length of 21.00 cm. The pyrolysis of α-cellulose was done in the same reactor by heating the α-cellulose at 600 °C for 3 h with an N_2 stream (20 mL/min) provided by PT. Samator Indonesia with 99.00% purity. During the hydrocracking of pyrolyzed α-cellulose, the catalyst to feed ratio of 1:30 was placed in the reactor. The reactor was then streamed by H_2 gas with a 20 mL/min flow rate and heated at 450 °C for 2 h. The obtained liquid was collected in the heart-shaped flask before it was characterized by using Gas Chromatography-Mass Spectroscopy (Shimadzu QP2010S).

2.3. Catalyst Characterizations

The acidity of the catalysts was tested by the gravimetric method using NH_3 gas as a basic adsorbate. The amount of cobalt present in the catalyst was determined by using an atomic absorption spectrophotometer (Perkin Elmer PinAAcle 900 T). The amorphous structure of SBA-15 was analyzed by an X-ray Diffractometer (Rigaku Miniflex 600) using Cu Kα radiation (0.154060 Å). The measurement conditions were in the range of 2θ = 20–80°. The particle sizes of Co and CoO can be calculated by using the Scherrer equation. The morpholo-

gy of the catalyst surface was characterized by using Scanning Electron Microscope - Energy Dispersive Spectroscopy (JEOL JED 2300) with an electron beam of 15.0 kV. TEM images were determined by a JEOL-JEM-1400 microscope with an electron beam of 120 kV. The pore characteristics (Brunauer–Emmett–Teller) of the catalysts were tested by using a gas adsorption analyzer (Quantachrome NovaWin version 11.0). The pore analysis was conducted using N_2 gas at 77.3 K.

2.4. Liquid Product Characterization

The obtained liquid was collected in the heart-shaped flask before it was characterized by using Gas Chromatography-Mass Spectroscopy (Shimadzu QP2010S). Method used for the measurement was: carrier gas of He (40 mL/min), injection mode (split), injection temperature of 310 °C, oven temperature program (started 50 °C (hold 5 min), finished 300 °C (hold 15 min, 5 mL/min)).

3. Results and Discussion

3.1. Catalyst Characterizations

During the catalyst preparation, the only difference between wet and co-impregnation was the addition of ethylene glycol to the cobalt aqueous solution prior to the dispersion on SBA-15 in the latter method. The deposition of cobalt on the mesoporous SBA-15 was due to capillary pressure [29]. However, the incomplete hydrophilicity of SBA-15 might cause incomplete wetting and inhomogeneous dispersion on pores [30]. Ethylene glycol assisted impregnation was reported to act as a surfactant and allow to decrease the surface tension of the aqueous solution that resulted in a better wetting of the support [21,22].

In line with previously reported work [21] the loading of metal (Co) on SBA-15 increases the acidity of the catalyst due to the Lewis acid sites provided by cobalt which acts as an electron which acts as an electron acceptor. As presented in Table 1, the reduced forms of cobalt (Co) are having higher acidity than its oxide form (CoO) which was because the zero-valence cobalt has more orbitals to accept electrons and consequently has higher acidity. Additionally, the higher loading of cobalt resulted in higher acidity of the solid catalyst.

The gas sorption analysis on the catalyst shows that the impregnation of cobalt on SBA-15 decreases the specific surface area and pore volume of SBA-15 that might be caused by the shrinkage of silica walls by the heat treatment of partial blockage of the mesoporous channel by the metal particles. The higher surface area of the impregnated catalysts prepared by co-impregnation was detected which might be indicating that the smaller particles of cobalt were formed. There will be a lower chance of pore-blocking when the smaller metal particles were deposited on the catalyst support that led to a higher specific surface area.

The impregnation of cobalt into SBA-15 gives peaks that characterized the presence of CoO and Co in the catalysts using XRD presented in Figure 1. The characteristic peaks of

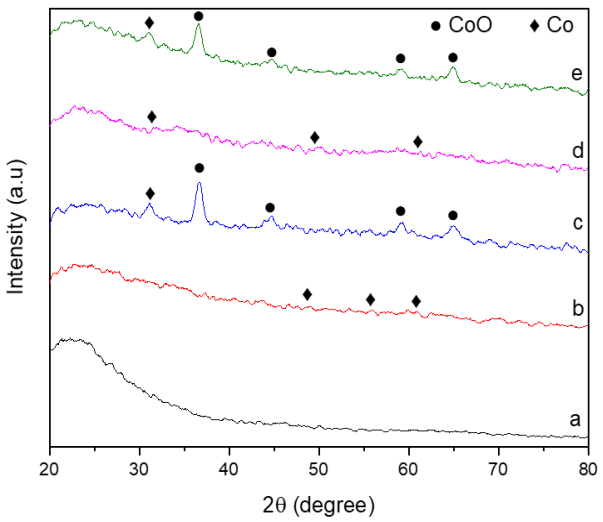

Figure 1. XRD pattern of (a) SBA-15, (b) Co/SBA-15c, (c) CoO/SBA-15c, (d) Co/SBA-15w, (e) CoO/SBA-15w catalysts.

Table 1. Physical and chemical properties of the catalysts.

Samples	Cobalt loading[a] (wt%)	Acidity[b] (mmole.g^{-1})	S_{BET}[c] (m^2.g^{-1})	Pore volume[c] (cm^3.g^{-1})	Average pore diameter[c] (nm)
SBA-15	-	3.99	623.8	1.05	6.75
CoO/SBA-15w	7.54	4.16	341.1	0.78	9.17
CoO/SBA-15c	6.28	4.23	393.1	0.72	7.36
Co/SBA-15w	6.43	6.33	337.7	0.76	8.96
Co/SBA-15c	7.97	7.42	432.3	0.78	7.19

[a] Cobalt loadings were determined by Atomic Absorption Spectrophotometer.
[b] Acidity of the catalysts were determined gravimetrically using NH_3 gas as a basic adsorbate.
[c] S_{BET} and pore volumes and diameters of the catalysts were calculated using BET and BJH theory, respectively.

CoO [31] could be found at 2θ approximately 36°, 42°, 61°, 73°, and 77°, while the peaks for Co [32] could be found at 2θ approximately 33°, 44°, 48°, 52°, 55°, and 61°. The CoO peak for both co-impregnation and wet impregnation shows strong peaks. During data processing, shifting of peaks might occur. The relatively weaker and more diffuse diffraction peaks were observed in Co/SBA-15c which indicates that the smaller particle size was generated via co-impregnation.

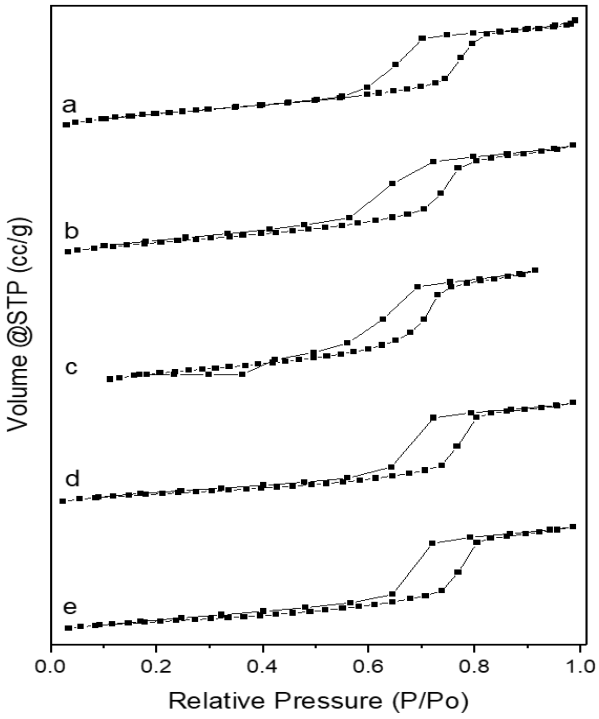

Figure 2. Adsorption/desorption isotherm of N_2 gas of (a) SBA-15, (b) Co/SBA-15c, (c) CoO/SBA-15c, (d) Co/SBA-15w, (e) CoO/SBA-15w catalysts.

The plot of adsorption and desorption isotherm of N_2 presented in Figure 2 shows that the catalyst was typical of a reversible type IV with hysteresis loops due to the mesoporous materials based on IUPAC classification. There were some changes in the shape of the graph after the impregnation of metal. This indicates that the impregnation of metal into the SBA-15 changes the pore characteristic of the catalyst. The wet impregnation showed more differences in the graph compared to the co-impregnation even though the graph of both methods is still considered as the mesoporous material.

According to the TEM images presented in Figure 3, the catalysts prepared through wet and co-impregnation show very clear distinctions. The catalyst prepared by wet impregnation (3b and d) shows large aggregates of cobalt particles on the external surface of SBA-15 due to their inability to enter the channels. This result was in line with that of nickel catalyst [22] we previously reported. This happened because the water as a solvent was unable to suppress the redistribution and agglomeration during

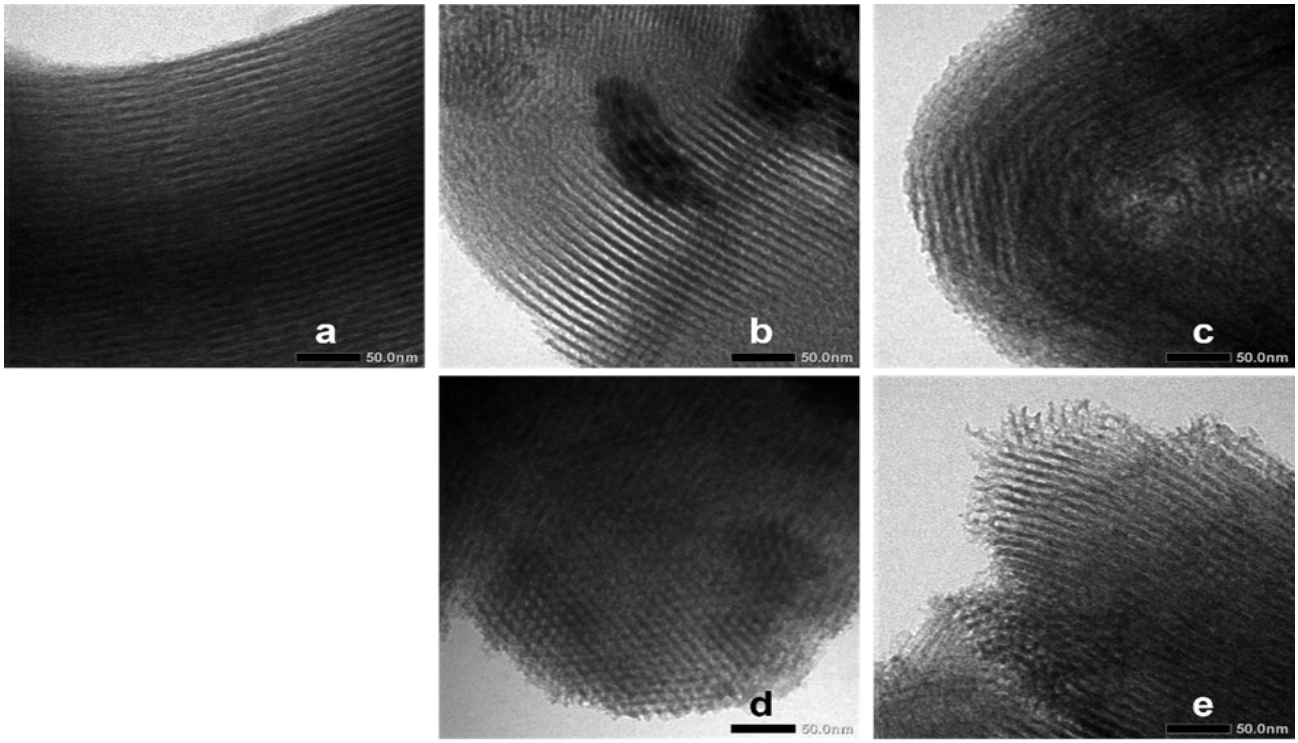

Figure 3. TEM images of (a) SBA-15, (b) CoO/SBA-15w, (c) CoO/SBA-15c, (d) Co/SBA-15w, (e) Co/SBA-15c catalysts.

the drying, calcination, and reduction process which resulted in the inhomogeneous distributions of cobalt particles. On the other hand, in the presence of EG, the cobalt particles were anchored inside the SBA-15 which resulted in a homogeneous and suppressing the particles growth and improve the resistance to coking and sintering [22].

3.2. Catalytic Activity on the Hydrocracking of Pyrolyzed α-Cellulose

The prepared catalysts were evaluated on the hydrocracking of pyrolyzed α-cellulose. α-cellulose was liquefied through pyrolysis prior to the hydrocracking process. The pyrolysis products were including char, an incondensable gas fraction, a condensable vapor composed of a complex mixture of organic compounds as shown in Table 2.

The cellulosic bio-oil comprised of anhydrosugars, furans, light oxygenates and pyrans [33]. The obtained bio-oil which is presented as a clear yellow organic liquid with a smoky odor was predominantly composed of carboxylic acid compounds, ketones, and furan compounds which correspond to the former investigation [34]. The yellow liquid was turned into a dark

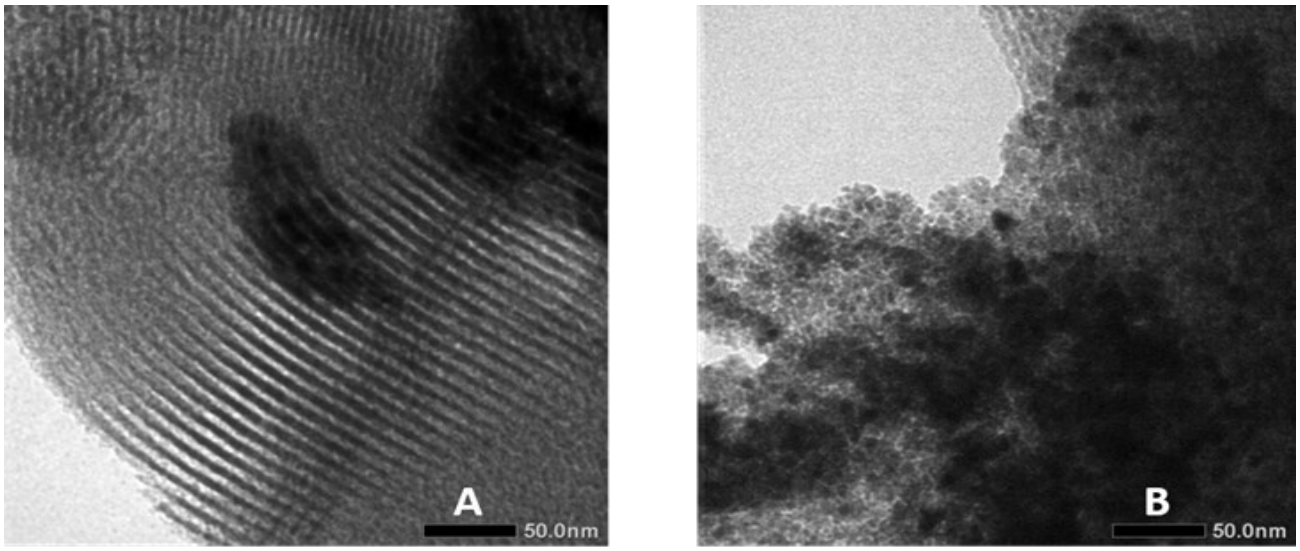

Figure 4. TEM image of Co/SBA-15w (a) before and (b) after hydrocracking.

Table 2. Major products of pyrolyzed α-cellulose based on GC-MS data [16].

Content (wt%)	Name	Molecular Formula
7.20	Formic acid	CH_2O_2
9.44	2,3-Butanedione	$C_4H_6O_2$
6.82	Acetic acid	$C_2H_4O_2$
10.27	1-Hydroxy-2-Propanone	$C_3H_6O_2$
2.51	Oxirane (butoxymethyl)	$C_7H_{14}O_2$
2.78	1-Hydroxy-2-Butanone	$C_4H_8O_2$
4.49	2-Furancarboxaldehyde	$C_5H_4O_2$
2.12	2-Furanmethanol	$C_5H_6O_2$

Table 3. Product distribution of hydrocracking process.

Catalyst	Cobalt particle size (nm)	Hydrocracking Product			Liquid fraction per Co loading
		Liquid Fraction (wt%)	Gas Fraction (wt%)	Coke (wt%)	
Thermal	-	48.61	51.39	0.00	-
SBA-15	-	70.89	28.81	0.30	-
CoO/SBA-15w	8.94	60.91	38.65	0.44	8.08
CoO/SBA-15c	7.17	63.66	36.09	0.25	10.14
Co/SBA-15w	7.05	72.72	26.39	0.90	11.31
Co/SBA-15c	0.60	70.37	29.53	0.10	8.83

as time goes by due to the polymerization proceed during the aging of oil and oxidation. For this reason, the obtained bio-oil was composed of unstable compounds.

The catalytic hydrotreating of the pyrolyzed α-cellulose gave a more stable liquid because the hydrotreating process can supply H_2 gas into the reactor and reduce the amount of oxygen present in the bio-oil. The product distribution of the hydrotreating process is shown in Table 3. The one with the lowest liquid fraction production was the thermal hydrotreating which was without using any catalyst and the highest production of the liquid fraction was the catalytic hydrotreating using Co/SBA-15w catalyst which also has the highest value of liquid fraction per Co loading. As shown in the Table 3, the CoO-based catalysts were producing less desired-liquid fraction with *ca.* 10% difference with the Co-based catalysts. As expected, the metallic species will be more active for this process. Moreover, the Co-based catalysts are having highest selectivity towards the production of highly valuable furfural.

In terms of coke resistance, the catalyst prepared by co-impregnation was indeed showing higher resistance towards the formation of coke which was in line with the previous reports [21,22]. Figure 4 shows the TEM images of Co/SBA-15w before and after hydrocracking. It is clearly shown that the deposition of coke on the catalyst support was inevitable despite its highest production of liquid fraction. However, the coke produced on Co/SBA-15w was still lower compared to the reported nickel-based catalyst [22].

The selectivity of liquid products grouped into aldehydes, ketones, carboxylic acids, and esters compounds are shown in Table 4. Based on Table 4, Co/SBA-15w and Co/SBA-15c were relatively having higher selectivity towards the production of acetic acid and 2-Furancarboxaldehyde. In this case, the conversion of biomass modeled by α-cellulose allowed to valorize the biomass source into more valuable chemicals like acetic acid which has a wide area of use. Moreover, the catalyst with the highest activity (Co/SBA-15w) showed the

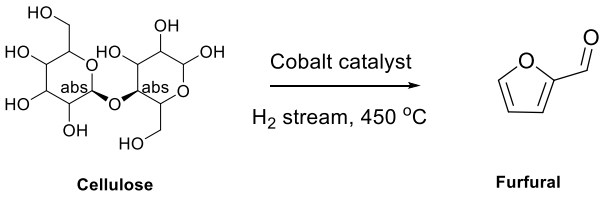

Scheme 1. Transformation of cellulose to versatile furfural.

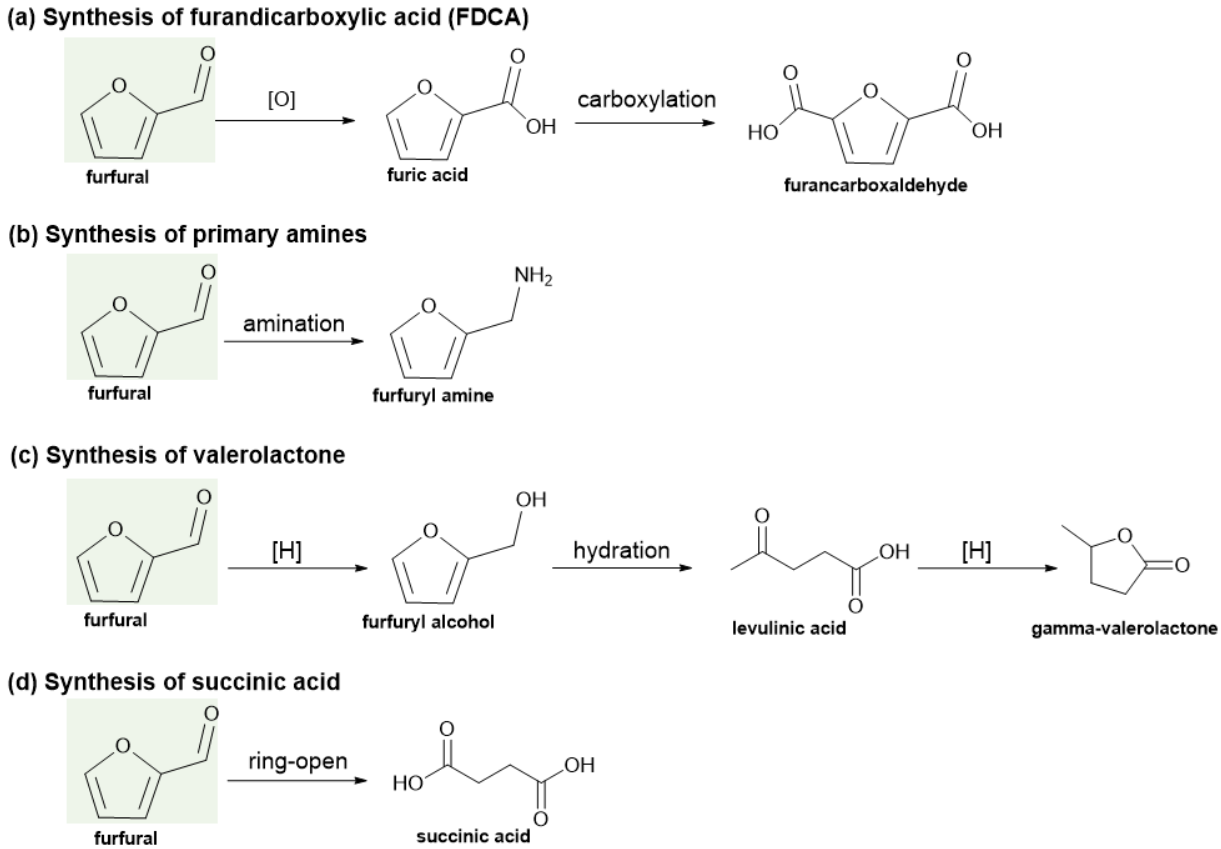

Scheme 2. Several diversifications of furfural in chemical industry.

highest selectivity towards the formation of 2-furancarboxaldehyde or furfural which is useful for the production of resins, abrasive wheels, and refractories, refining of lubrication oils, and solvent recovery (Scheme 1). This is interesting that the selectivity towards the hydrocracking products could be differ as the metal change as compared to our previous work [22]. This is probably due to the interaction between the metal and support material could direct the catalytic performance on the final product. As we know that furfural is a reactive chemical that can be use for a lot of value-added chemicals and liquid fuels [35–37]. For instances (Scheme 2), it act as a precursor to form FDCA that can be used in the polyethylene terephthalate (PET) industry to produce biodegradable plastic materials as a greener alternative [3]. Moreover, highly useful biomass-derived chemical building blocks such as furfuryl amines, furfuryl alcohols, as well as succinic acid and gamma-valerolacton could be generated by chemical transformation of furfural.

4. Conclusions

The preparation of heterogeneous catalysts based on cobalt supported on SBA-15 were performed through wet and co-impregnation assisted by EG. The TEM images revealed the catalysts prepared through these methods show very clear distinctions that the catalyst prepared by assistance of ethylene glycol allowed to generate smaller Co particle. However, the catalyst prepared by co-impregnation (Co/SBA-15c) showed slightly lower catalytic activity despite its smaller particle size and higher coke resistance compared to that prepared by wet impregnation (Co/SBA-15w). The catalyst with the highest activity (Co/SBA-15w) showed the highest selectivity towards the formation of 2-furancarboxaldehyde which is useful for the production of resins, abrasive wheels, and refractories, refining of lubrication oils, and solvent recovery.

Acknowledgments

The authors thank Ministry of Research Technology and Higher Education/National Research Council (KEMENRISTEK/BRIN) Republic of Indonesia for the financial support under the scheme of PDUPT research grant 2021 (Contract Number: 6/E1/KP.PTNBH/2021).

References

[1] Bridgwater, A.V. (2003). Renewable fuels and chemicals by thermal processing of biomass. *Chemical Engineering Journal,* 91(2-3), 87–102. DOI: 10.1016/S1385-8947(02)00142-0

[2] Vassilev, S.V., Baxter, D., Andersen, L.K., Vassileva, C.G. (2013). An overview of the composition and application of biomass ash.: Part 2 Potential utilisation, technological and ecological advantages and challenges. *Fuel,* 105, 19–39. DOI: 10.1016/j.fuel.2012.10.001

[3] Pandey, A., Bhaskar, T., Stöcker, M., Sukumaran, R. (2015). *Recent Advances in Thermochemical Conversion of Biomass*. Boston: Elsevier. DOI: 10.1016/C2013-0-00403-3

[4] Tan, Z., Chen, K., Liu, P. (2015). Possibilities and challenges of China's forestry biomass resource utilization. *Renewable and Sustainable Energy Reviews,* 41, 368–378. DOI: 10.1016/j.rser.2014.08.059

[5] Nomiyama, T., Aihara, N., Chitose, A., Yamada, M., Tojo, S. (2014). *Biomass as local resource: Research approaches to sustainable biomass systems*. Boston: Academic Press.

[6] Xiao, L., Zhang, Q., Chen, P., Chen, L., Ding, F., Tang, J., Li, Y.J., Au, C.T., Yin, S.F. (2019). Copper-mediated metal-organic framework as efficient photocatalyst for the partial oxidation of aromatic alcohols under visible-light irradiation: Synergism of plasmonic effect and schottky junction. *Applied Catalysis B: Environmental*, 248, 380–387. DOI: 10.1016/j.apcatb.2019.02.012

[7] Xiang, Z., Liang, J., Morgan Jr, H.M., Liu, Y., Mao, H., Bu, Q. (2018). Thermal behavior and kinetic study for co-pyrolysis of lignocellulosic biomass with polyethylene over Cobalt modified ZSM-5 catalyst by thermogravimetric analysis. *Bioresource Technology*, 247, 804–811. DOI: 10.1016/j.biortech.2017.09.178

[8] Bu, Q., Chen, K., Xie, W., Liu, Y., Cao, M., Kong, X., Chu, Q., Mao, H. (2019). Hydrocarbon rich bio-oil production, thermal behavior analysis and kinetic study of microwave-assisted co-pyrolysis of microwave-torrefied lignin with low density polyethylene. *Bioresource Technology*, 291, 121860. DOI: 10.1016/j.biortech.2019.121860

[9] Kobayashi, H., Komanoya, T., Guha, S.K., Hara, K., Fukuoka, A. (2011). Conversion of cellulose into renewable chemicals by supported metal catalysis. *Applied Catalysis A: General,* 409–410, 13–20. DOI: 10.1016/j.apcata.2011.10.014

[10] Anwar, Z., Gulfraz, M., Irshad, M. (2014). Agro-industrial lignocellulosic biomass a key to unlock the future bio-energy: A brief review. *Journal of Radiation Research and Applied Sciences,* 7(2), 163–173. DOI: 10.1016/j.jrras.2014.02.003

[11] Mika, L.T., Csefalvay, E., Nemeth, A. (2018). Catalytic Conversion of Carbohydrates to Initial Platform Chemicals: Chemistry and Sustainability. *Chemical Reviews*, 118(2), 505–613. DOI: 10.1021/acs.chemrev.7b00395

[12] Xiu, S., Shahbazi, A. (2012). Bio-oil production and upgrading research: A review. *Renewable and Sustainable Energy Reviews,* 16(7), 4406–4414. DOI: 10.1016/j.rser.2012.04.028

[13] Chen, S., Wojcieszak, R., Dumeignil, F., Marceau, E., Royer, S. (2018). How Catalysts and Experimental Conditions Determine the Selective Hydroconversion of Furfural and 5-Hydroxymethylfurfural. *Chemical Reviews*, 118(22), 11023–11117. DOI: 10.1021/acs.chemrev.8b00134

[14] Hong, M., Min, J., Wu, S., Li, J., Wang, J., Wei, L., Ling, Z., Li, K., Wang, S. (2020). Functionalized expanded corn starch-anchored Cu(I): An efficient and recyclable catalyst for oxidation of 5-hydroxymethylfurfural to 2,5-diformylfuran. *Applied Organometallic Chemistry*, 34(3), e5411. DOI: 10.1002/aoc.5411

[15] Yu, F.W., Ji, D.X., Nie, Y., Luo, Y., Huang, C.J., Ji, J.B. (2012). Study on The Pyrolysis of Cellulose for Bio-oil with Mesoporous Molecular Sieve Catalysts. *Applied Biochemistry and Biotechnology,* 168, 174–182. DOI: 10.1007/s12010-011-9398-5

[16] Grams, J., Potrzebowska, N., Goscianska, J., Michalkiewicz, B., Ruppert, A.M. (2016). Mesoporous silicas as supports for Ni catalyst used in cellulose conversion to hydrogen rich gas. *International Journal of Hydrogen Energy,* 41, 8656–8667. DOI: 10.1016/j.ijhydene.2015.12.146

[17] Perego, C., Bosetti, A. (2013). Biomass to fuels: The role of zeolite and mesoporous materials. *Microporous and Mesoporous Materials,* 144, 28–39. DOI: 10.1016/j.micromeso.2010.11.034

[18] Wang, C.X., Yang, F., Yang, W., Ren, L., Zhang, Y.H., Jia, X., Zhang, L.Q., Li, Y.F. (2015). PdO nanoparticles enhancing the catalytic activity of Pd/carbon nanotubes for 4-nitrophenol reduction. *RSC Advances,* 5, 27526–27532. DOI: 10.1039/C4RA16792A

[19] Lin, S., Shi, L., Carrott, M.M.L.R., Carrott, P.J.M., Rocha, J., Li, M.R., Zou, X.D. (2011). Direct synthesis without addition of acid of Al-SBA-15 with controllable porosity and high hydrothermal stability. *Microporous and Mesoporous Materials*, 142(2-3), 526–534. DOI: 10.1016/j.micromeso.2010.12.043

[20] Tao, M., Sin, Z., Meng, X., Bian, Z., Lv, Y. (2017). Highly dispersed nickel within mesochannels of SBA-15 for CO methanation with enhanced activity and excellent thermostability. *Fuel,* 188, 267–276. DOI: 10.1016/j.fuel.2016.09.081

[21] Lu, J., Fu, B., Kung, M.C., Xiao, G., Elam, J.W., Kung, H.H., Stair, P.C. (2012). Coking- and Sintering-Resistant Palladium Catalysts Achieved Through Atomic Layer Deposition. *Science,* 335, 1205–1208. DOI: 10.1126/science.1212906

[22] Trisunaryanti, W., Suarsih, E., Triyono, T., Falah, I.I. (2019). Well-dispersed nickel nanoparticles on the external and internal surfaces of SBA-15 for hydrocracking of pyrolyzed α-cellulose. *RSC Advances,* 9, 1230–1237. DOI: 10.1039/C8RA09034C

[23] Qiu, S., Zhang, Q., Lv, W., Wang, T., Zhang, Q., Ma, L. (2017). Simply packaging Ni nanoparticles inside SBA-15 channels by co-impregnation for dry reforming of methane. *RSC Advances*, 7, 24551–24560. DOI: 10.1039/C7RA00149E

[24] Xie, T., Shi, L.Y., Zhang, J.P., Zhang, D.S. (2014). Immobilizing Ni nanoparticles to mesoporous silica with size and location control via a polyol-assisted route for coking- and sintering-resistant dry reforming of methane. *Chemical Communications,* 50, 7250–7253. DOI: 10.1039/C4CC01441C

[25] Lv, X.Y., Chen, J.F., Tan, Y.S., Chang, Y. (2012). A highly dispersed nickel supported catalyst for dry reforming of methane. *Catalysis Communications,* 20, 6–11. DOI: 10.1016/j.catcom.2012.01.002

[26] Liu, D.P., Quek, X.Y., Cheo, W.N.E., Lau, R., Borgna, A., Yang, Y.H. (2009). MCM-41 supported nickel-based bimetallic catalysts with superior stability during carbon dioxide reforming of methane: Effect of strong metal–support interaction. *Journal of Catalysis,* 266(2), 380–390. DOI: 10.1016/j.jcat.2009.07.004

[27] Bechara, R., Balloy, D., Vanhove, D. (2001). Catalytic properties of Co/Al_2O_3 system for hydrocarbon synthesis. *Applied Catalysis A: General,* 207(1-2), 343–353. DOI: 10.1016/S0926-860X(00)00672-4

[28] Sohn, H., Ozkan, U.S. (2016). Cobalt-based Catalysts for Ethanol Steam Reforming: An Overview. *Energy and Fuels,* 30(7), 5309–5322. DOI: 10.1021/acs.energyfuels.6b00577

[29] Munnik, P., De Jongh, P.E., De Jong, K.P. (2015). Recent developments in the synthesis of supported catalysts. *Chemical Reviews,* 115(14), 6687–6718. DOI: 10.1021/cr500486u

[30] Sietsma, J.R.A., Meeldijk, J.D., et al. (2008) Ordered mesoporous silica to study the preparation of Ni/SiO_2 ex nitrate catalysts: impregnation, drying, and thermal treatments. *Chemistry of Materials,* 20(9), 2921–2931. DOI: 10.1021/cm702610h

[31] Barakat, N.A.M., Khil, M.S., Sheikh, F.A., Kim, H.Y. (2008). Synthesis and optical properties of two cobalt oxides (CoO and Co_3O_4) nanofibers produced by electrospinning process. *The Journal of Physical Chemistry C,* 112(32), 12225–12233. DOI: 10.1021/jp8027353

[32] Mishra, A., Jain, G., Ninama, S. (2014). Surface, morphology, and X-ray diffraction studies of Co (II) complexes of pyrazole ligands. *Journal of Physics: Conference Series,* 534, 012034. DOI: 10.1088/1742-6596/534/1/012034

[33] Ansari, K.B., Arora, J.S., Chew, J.W., Dauenhauer, P.J., Mushrif, S.H. (2019). Fast Pyrolysis of Cellulose, Hemicellulose, and Lignin: Effect of Operating Temperature on Bio-oil Yield and Composition and Insights into the Intrinsic Pyrolysis Chemistry. *Industrial & Engineering Chemistry Research,* 58(35), 15828–15852. DOI: 10.1021/acs.iecr.9b00920

[34] Santos, R.M., Santos, A.O., Sussuchi, E.M., Nascimento, J.S., Lima, A.S., Freitas, L.S. (2015). Pyrolysis of mangaba seed: production and characterization of bio-oil. *Bioresource Technology,* 196, 43–48. DOI: 10.1016/j.biortech.2015.07.060

[35] Bohre, A., Dutta, S., Saha, B., Abu-Omar, M.M. (2015). Upgrading furfurals to drop-in biofuels: an overview. *ACS Sustainable Chemistry & Engineering*, 3, 1263–1277. DOI: 10.1021/acssuschemeng.5b00271

[36] Yan, K., Wu, G., Lafleur, T., Jarvis, C. (2014). Production, properties and catalytic hydrogenation of furfural to fuel additives and value-added chemicals. *Renewable and Sustainable Energy Reviews*, 38, 663–676. DOI: 10.1016/j.rser.2014.07.003

[37] Buntara, T., Noel, S., Phua, P.H., Melián-Cabrera, I., De Vries, J.G., Heeres, H.J. (2011). Caprolactam from renewable resources: Catalytic conversion of 5-hydroxymethylfurfural into caprolactone. *Angewandte Chemie International Edition*, 50, 7083–7087. DOI: 10.1002/anie.201102156